METHODS IN ENZYMOLOGY

EDITORS-IN-CHIEF

John N. Abelson Melvin I. Simon

DIVISION OF BIOLOGY
CALIFORNIA INSTITUTE OF TECHNOLOGY
PASADENA, CALIFORNIA

FOUNDING EDITORS

Sidney P. Colowick and Nathan O. Kaplan

Methods in Enzymology

Volume 336

Microbial Growth in Biofilms

Part A

Developmental and Molecular Biological Aspects

EDITED BY

Ron J. Doyle

UNIVERSITY OF LOUISVILLE
LOUISVILLE, KENTUCKY



ACADEMIC PRESS

San Diego London Boston New York Sydney Tokyo Toronto

Yr 2001

[24] Characterization of Extracellular Chitinolytic Activity in Biofilms

By ACE M. BATY III, ZHENJUN DIWU, GLEN DUNHAM, CALLIE C. EASTBURN, GILL G. GEESEY, AMANDA E. GOODMAN, PETER A. SUCI, and SOMKIET TECHKARNJANARUK

Introduction

It is common for bacteria to produce extracellular enzymes having some form of degradative activity. In some cases these enzymes serve to protect cells from antagonistic substances,[1–3] or to convert a large and/or insoluble biopolymer to an assimilable nutrient source.[4,5] In some cases the physiological benefit to the bacterium is not entirely evident.[6,7] Extracellular enzymes may be membrane bound, but in many cases they are released into the surrounding medium.[8] It has been shown that these relatively large molecules become immobilized in the extracellular polymeric matrix in which cells in flocs and biofilms are embedded.[9] Most proteins adsorb irreversibly to substrata having a variety of surface chemistries,[10] and transport by convection is reduced near any solid surface, regardless of the flow regimen in the bulk liquid.[11] Thus, extracellular enzymes have a tendency to become an integral and significant component of the biofilm/substratum microenvironment, influencing cell physiology and biofilm ecology.

In this chapter methods for characterizing extracellular enzyme activity associated with biofilms are presented. There are three components of the methodology. The first is a precipitating fluorogenic enzyme substrate (ELF-97-*N*-acetyl-β-D-glucosaminide) (ELF-NAG),* used to localize extracellular catalytic activity.

[1] G. Harth and M. A. Horwitz, *J. Biol. Chem.* **274,** 4281 (1999).
[2] J. M. Frere, *Mol. Microbiol.* **16,** 385 (1995).
[3] A. Kharazmi, *Immunol. Lett.* **30,** 201 (1991).
[4] E. A. Bayer, L. J. Shimon, Y. Shoham, and R. Lamed, *J. Struct. Biol.* **124,** 221 (1998).
[5] G. P. Hazlewood and H. J. Gilbert, *Prog. Nucleic Acid Res. Mol. Biol.* **61,** 211 (1998).
[6] R. J. Lamont and H. F. Jenkinson, *Microbiol. Mol. Biol. Rev.* **62,** 1244 (1998).
[7] M. J. Benedik and U. Strych, *FEMS Microbiol. Lett.* **165,** 1 (1998).
[8] R. G. Wetzel, *in* "Microbial Enzymes in Aquatic Environments" (R. J. Chrost, ed.), p. 6. Springer-Verlag, New York, 1991.
[9] B. Frolund, T. Griebe, and P. H. Nielsen, *Appl. Microbiol. Biotechnol.* **43,** 755 (1995).
[10] J. D. Andrade, *in* "Surface and Interfacial Aspects of Biomedical Polymers," Vol. 2: "Protein Adsorption" (J. D. Andrade, ed.), p. 1. Plenum Press, New York, 1985.

*ELF-97 is a registered trademark used by the company Molecular Probes (Eugene, OR). ELF is an acronym for enzyme-labeled fluorescence. We use ELF to refer to the precipitating fluorophore produced by enzyme cleavage: 2-(2′-hydroxy-5′-chlorophenyl)-6-chloro-4(3*H*)-quinazolinone.[11a]

Copyright © 2001 by Academic Press
All rights of reproduction in any form reserved.
0076-6879/00 $35.00

Similar methodologies have been used to probe enzyme activity in biofilms[12] and microbial flocs.[13] ELF-NAG is soluble and nonfluorescent until it is cleaved by the enzyme. Once cleaved, one of the products fluoresces and precipitates onto the substratum. Because the soluble substrate cannot enter the cell, the assay indicates activity of extracellular enzymes exclusively.** Additional information is obtained by using green fluorescent protein (GFP) to report promoter (transcriptional) activity of relevant genes using established techniques.[14]

The second component of the methodology is the use of thin films to fabricate a substratum with properties that mimic a natural surface, but allow cells and fluorescent areas to be detected by conventional light microscopy with micron spatial resolution. Many relevant natural surfaces are either too rough and/or fluoresce too strongly to enable this level of resolution by conventional microscopy. Therefore, elaborate and time-consuming methodologies must be applied to characterize biofilms on these surfaces.[15] Incorporation of thin films into an *in vitro* system allows relevant hypotheses about the natural system to be addressed by relatively simple methods. Spin-casting a substance onto a planer surface produces films that are optically smooth, and so thin (e.g., 50 nm) that the fluorescence from the material is a negligible background. The method is relatively simple, requiring only that a volatile solvent for the substance can be found.

The third component of the methodology is a spin-off of the use of thin films. There are a number of well-established techniques that can be used to characterize thin films under hydrated conditions nondestructively, in real time. These include the quartz crystal microbalance,[16] surface plasmon resonance,[17] total internal reflection fluorescence,[18] and attenuated total reflection Fourier transform

[11] S. Vogel, "Life in Moving Fluids," pp. 127–162. Princeton University Press, Princeton, New Jersey, 1981.

[11a] K. D. Larison, R. BreMiller, S. Wells, I. Clements, and R. P. Haugland, *J. Histochem. Cytochem.* **43,** 77 (1995).

[12] C. T. Huang, K. D. Xu, G. A. McFeters, and P. S. Stewart, *Appl. Environ. Microbiol.* **64,** 1526 (1998).

[13] F. Van Ommen Kloeke and G. G. Geesey, *Microb. Ecol.* **38,** 201 (1999).

[14] B. B. Christensen, C. Sternberg J. B. Andersen, R. J. Palmer, Jr., A. T. Nielsen, M. Givskov, and S. Molin, *Methods Enzymol.* **310,** 20 (1999).

[15] B. Normander, N. B. Hendriksen, and O. Nybroe, *Appl. Environ. Microbiol.* **65,** 4646 (1999).

[16] H. Ebato, C. A. Gentry, J. N. Herron, W. Muller, Y. Okahata, H. Ringsdorf, and P. A. Suci, *Anal. Chem.* **66,** 1683 (1994).

[17] W. Knoll, W. Hickel, M. Sawodny, J. Stumpe, and H. Knobloch, *Fresenius J. Anal. Chem.* **341,** 272 (1990).

[18] Y.-L. Cheng, B. K. Lok, and C. R. Robertson, *in* "Surface and Interfacial Aspects of Biomedical Polymers," Vol. 2: "Protein Adsorption" (J. D. Andrade, ed.), p. 121. Plenum Press, New York, 1985.

**Our results indicate that ELF-NAG does not enter into the cytoplasm of *Pseudoalteromonas* sp. strain S91. However, it may penetrate into other types of bacteria.

infrared spectroscopy (ATR-FTIR).[19] Using one or more of these techniques, it is possible, in principle, to measure degradation of the thin film by an associated biofilm. In the special case where the thin film incorporates a substrate for an extracellular enzyme, the chosen technique can provide a measure of the kinetics of substrate degradation. We have designed an *in vitro* system that enables both microscopic images and ATR-FTIR data to be acquired from a biofilm under flowing conditions.[20]

The success of the methods outlined above is demonstrated here, using results obtained from a chitinolytic marine bacterium, *Pseudoalteromonas* sp. strain S91 (S91) cultured on thin films of chitin.[21–23] Degradation of particulate organic matter (POM) in the ocean is one of the processes that has a major influence on the global ecology. Bacteria are thought to contribute significantly to degradation of POM.[24–26] The associated ecological system has been termed the microbial loop.[27] POM is, of course, too large to enter bacterial cells, and even the component biopolymers are, in general, not cell permeable. Therefore, bacterial extracellular enzymes are an essential component of the microbial loop.[28] Bacterial chitinolytic enzymes are thought to be chiefly responsible for the conversion of the enormous marine chitin reservoir into dissolved organic matter (DOM).[29] Although extracellular enzymes produced by bacterial biofilms undoubtedly make a significant contribution to carbon cycling,[30] there is a paucity of data providing direct information about marine biofilms associated with POM. A significant obstacle to acquiring this data has been methodological, i.e., overcoming the difficulties associated with detection of single cells on relevant natural surfaces.

Bacteria capable of hydrolyzing high molecular weight chitin are widely distributed in sediments, on the surface of plants, in the gut of marine mammals, and

[19] K. Knutzen and D. J. Lyman, *in* "Surface and Interfacial Aspects of Biomedical Polymers," Vol. 1: "Surface Chemistry and Physics" (J. D. Andrade, ed.), p. 197. Plenum Press, New York, 1985.

[20] P. A. Suci, K. J. Siedleki, R. J. Palmer, Jr., D. C. White, and G. G. Geesey, *Appl. Environ. Microb.* **63,** 4600 (1997).

[21] A. M. Baty, Physiological Diversity of an Attached Marine Bacterial Population," pp. 1–142. Ph.D. Thesis, Montana State University, Bozeman, Montana, 1999.

[22] A. M. Baty, C. C. Eastburn, Z. Diwu, S. Techkarnjanaruk, A. E. Goodman, and G. G. Geesey, *Appl. Environ. Microbiol.* **66,** 3566 (2000).

[23] A. M. Baty, C. C. Eastburn, S. Techkarnjanaruk, A. E. Goodman, and G. G. Geesey, *Appl. Environ. Microbiol.* **66,** 3574 (2000).

[24] D. A. Caron, P. G. Davis, L. P. Madin, and J. M. Sieburth, *Science* **218,** 795 (1982).

[25] D. C. Smith, M. Simon, A. L. Alldredge, and F. Azam, *Nature (London)* **359,** 139 (1992).

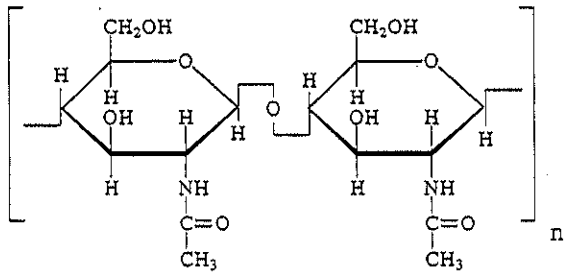
[26] F. Azam, *Science* **280,** 694 (1998).

[27] T. Berman and L. Stone, *Microb. Ecol.* **28,** 251 (1994).

[28] H. G. Hoppe, *in* "Microbial Enzymes in Aquatic Environments" (R. J. Chrost, ed.), p. 60. Springer-Verlag, New York, 1991.

[29] G. W. Gooday, *Biodegradation* **1,** 177 (1990).

[30] M. Karner and G. J. Herndl, *Mar. Biol.* **113,** 341 (1992).



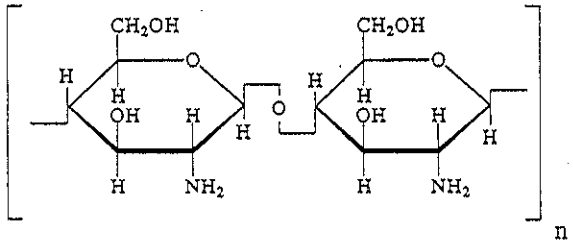


FIG. 1. Haworth projections of structures of chitin and chitosan. Chitosan is soluble in aqueous solution. Thin chitin films are formed by spin casting chitosan followed by acetylation of the films (described in text).

associated with POM.[31] These bacteria synthesize and export chitinase enzymes that can cleave the β-1,4-linkage of the homopolymer chitin (Fig. 1).[32] High molecular weight chitin is degraded into chitin oligomers by extracellular endochitinase. Oligomers are acted on by chitobiase to produce dimers of chitin that can be incorporated into the periplasm of bacteria. In the periplasm these dimers are cleaved into monomers by *N*-acetylglucosaminidases. In addition, extracellular exochitinases cleave single sugars off the reducing ends of the polymer chains. Extracellular *N*-acetylglucosaminidase can also be secreted and cleave small oligomers into monomers outside the cell. A single chitinolytic bacterium may express all these enzymes in an effort to efficiently utilize high molecular weight solid chitin. Figure 2 shows the activity and possible location of different chitinase enzymes with respect to a chitinolytic bacterium. S91 is a genetic construct in which GFP reports promoter activity of a gene (*chiA*) encoding an extracellular chitinase. ELF-NAG is cleaved both by exochitinase and *N*-acetylglucosaminidase

[31] C. E. Zobell and S. C. Rittenburg, *J. Bacteriol.* **35,** 275 (1937).
[32] M. B. Brurberg, I. F. Nes, and V. G. H. Eijsink, *in* "Chitin Enzymology," Vol. 2 (R. A. A. Muzzarelli, ed.), p. 171. Atec Edizioni, Ancona, Italy, 1996.

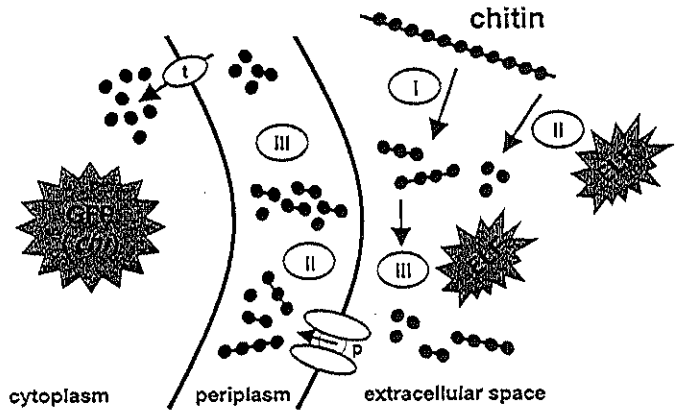


FIG. 2. Types of chitinolytic enzymes and possible locations with respect to a bacterium. I, Endochitinase; II, exochitinase; III, *N*-acetylglucosaminidase; p, porin; t, *N*-acetylglucosamine transporter; *chi*, gene for general chitinase enzyme. Sites of GFP and ELF-NAG fluorescence are indicated by GFP and ELF, respectively.

(Fig. 2). Although results suggest that *chiA* encodes an exochitinase,[21–23] this remains hypothetical because the enzyme has not been purified to homogeneity. Details of the genetic construct are given below and in the referenced literature.

Fabrication of Thin Films of Chitin

Published techniques were used to fabricate chitin films, with some modifications.[33–35] To our knowledge, chitin is not soluble in any volatile organic solvent. The protocol consists of casting films of chitosan onto a solid support and then converting the chitosan (Aldrich, Milwaukee, WI) to chitin by N-acetylation (see Fig. 1 for structures). Films are cast onto silicon coupons for the evaluation of bacterial gene expression, X-ray photoelectron spectroscopy (XPS) analysis, and profilometry; onto AT-cut quartz crystals for profilometry and mass determination by quartz crystal microbalance (QCM); and onto germanium (Ge) internal reflection elements (IREs) for infrared (IR) spectroscopy. Silicon coupons, 1 × 1 cm square (Harrick Scientific, Ossining, NY), are cleaned in "Piranha," which consists of a 70 : 30 mixture of concentrated sulfuric acid and 30% hydrogen peroxide (Piranha solution reacts violently, even explosively, with organic materials).[36] The silicon coupons are then rinsed in distilled H_2O and dried under

[33] H. Bae and S. M. Hudson, *J. Appl. Poly. Sci. A Poly. Chem.* **35,** 3755 (1997).
[34] T. D. Rathke and S. M. Hudson, *J. Mater. Sci. Rev. Macromol. Chem. Phys.* **C34,** 375 (1994).
[35] Y. Qin, *J. Appl. Poly. Sci.* **49,** 727 (1993).
[36] D. A. Dobbs, R. G. Bergman, and K. H. Theopold, *Chem. Eng. News* **68,** 2 (1990).

a stream of pure dry nitrogen. Quartz crystals are cleaned with a cotton-tipped applicator successively in water, methanol, and chloroform and dried under a stream of dry nitrogen. Single-crystal, Ge IREs (EJ 2121; Harrick Scientific) are cleaned by ultrasonication in a base bath (saturated KOH in isopropyl alcohol) for 10 min followed by a series of rinses, all of which consist of ultrasonication in various liquids for 10 min. After the base bath are two rinses in "ultrapure" water followed by a gentle scrubbing with undiluted Micro cleaning solution, using cotton swabs. The cleaning solution is flushed off in a hard stream of ultrapure water. The IRE is then subjected to the following rinses: ultrapure water (twice), ethyl alcohol, and chloroform. IREs are air dried at 100°.

Chitosan solutions are prepared in aqueous 2.0% (v/v) acetic acid and then filtered through a 0.2-μm syringe filter to remove any insoluble debris. Except for cleaning, the spin-casting protocols for silicon coupons and quartz crystals are identical. Coupons are affixed to the middle of a centrifuge rotor with double-stick tape, and scrubbed with methanol followed by chloroform, using cotton-tipped applicators. Approximately 300 μl of the chitosan solution is placed on the surface of the coupon and spun with rapid acceleration at 4500 rpm for 5 min. While the surface is still spinning the chitosan thin film is washed successively with 1.0 ml of 5.0% (w/v) NaOH, 10.0 ml of distilled H_2O, and 1.0 ml of methanol. Films are then dried in a desiccating chamber overnight. For N-acetylation, coupons are placed in 10.0 ml of ice-cold, dry methanol and 2.5 ml of ice-cold acetic anhydride is added with stirring. The reaction is allowed to proceed for 18 hr at 4°. Coupons are then rinsed in methanol four times and placed on the spin caster, where they are rinsed with an additional 10.0 ml of methanol while spinning at 3000 rpm. Films are dried overnight in a desiccating chamber. The protocol for making thin chitin films on a Ge IRE is the same as for silicon coupons except that the IRE is fixed to the centrifuge rotor by a Teflon holder designed to accommodate the Ge IRE during casting. It consists essentially of a block of Teflon with an appropriately sized cavity.

The quality of the chitin thin films decreases with increasing chitosan casting solution concentrations. Chitin thin films prepared from solutions containing more than 4% (w/v) chitosan cannot be constructed because of the high viscosity of the chitosan solutions. Chitin thin films prepared from solutions containing more than 2% (w/v) chitosan trap air bubbles during casting, resulting in usable films but with visually observable film defects. On the basis of visual observation, 1% (w/v) chitosan-cast chitin thin films appear to be continuous and evenly distributed. The most critical step in the construction of these films is the cleaning of the silicon substratum. The slightest residue can result in major defects in the thin film. On N-acetylation of the chitosan films, the resulting chitin film always appears slightly darker in color.

TABLE I
ATOMIC CONCENTRATION OF CHITOSAN AND CHITIN THIN FILMS

	Atomic concentration (%)		
	Carbon	Nitrogen	Oxygen
Chitosan thin film	46.19 ± 1.12	5.56 ± 0.91	48.25 ± 1.01
Chitin thin film	62.19 ± 1.23	6.18 ± 0.74	31.63 ± 0.89
Chitin (theoretical)	57.14	7.14	35.7

Characterization of Thin Films

The fluorescence of the thin films is evaluated by epifluorescence microscopy. Differential interference contrast (DIC) microscopy and profilometry are used to evaluate the continuity of the chitin thin films. Surface chemistry is quantified spatially by XPS. The density of the chitin thin films is determined by thickness measurements obtained by profilometry and mass measurements determined by QCM. ATR-FTIR is used to characterize film chemistry and crystal structure.

Atomic Composition by X-Ray Photoelectron Spectroscopy

XPS is performed with a Physical Electronics (Eden Prairie, MN) model 5600 spectrometer. A 5-eV flood gun is used to offset charge accumulation on the samples. An aperture of 30 μm is used with a monochromatized aluminum K_α X-ray source at 350 W and a pass energy of 11.750 eV. Survey spectra and high-resolution spectra are gathered at a take-off angle of 45°. Abundance of carbon, nitrogen, and oxygen is calculated from high-resolution C1s, N1s, and O1s peak areas. The binding energy scale is referenced by setting the CHx peak maximum in the C1s spectrum to 285.0 eV.[37] The atomic composition of three 30-μm spots on each of three chitin thin films prepared from a 1.5% (w/v) chitosan solution ($n = 9$) is evaluated (Table I). The atomic composition is presented as percent carbon, nitrogen, and oxygen with the standard error.

The atomic concentrations of carbon, nitrogen, and oxygen of the chitin thin films are similar to the theoretical concentrations for pure chitin (Table I). Differences may be attributed to surface hydrocarbon contamination. The standard error in atomic concentration displayed between a total of nine different 30-μm spots on three separately prepared chitin thin films ranges from 0.74 to 1.23%. These standard errors are within the range of anticipated reproducibility for XPS.

[37] B. D. Ratner and D. G. Castner, *in* "Surface Analysis–Techniques and Applications" (J. C. Vickerman and N. M. Reed, eds.), p. 163. John Wiley & Sons, Chichester, UK, 1994.

Therefore, the XPS measurements indicate that the films have a high degree of spatial homogeneity.

Thickness by Profilometry

Film thickness is determined for chitin thin films cast onto quartz crystals and onto silicon substrata, using profilometry.[38] White light (200 nm) is simultaneously reflected from the test surface and a reference surface and is recombined to produce a fringence pattern. A vertical scanning piezoelectric transducer synchronized with a charge-coupled device (CCD) camera and frame grabber generates interferograms of the surface and a computer translates these interferograms into a quantitative three-dimensional (3-D) image of surface topography. To obtain a film thickness from the 3-D profile of the surface, the chitin thin films are scored with a 27-guage needle down to the substratum. Because the chitin thin films are transparent, it is necessary to sputter-coat the surfaces with approximately 150 Å of gold. The depth of the score is then measured with a Zygo (Middlefield, CT) NEW View 200 profilometer to obtain the film thickness. A 20× objective is used to obtain data with a vertical resolution of 0.1 nm and a lateral resolution of 0.64 μm. Data are collected at a scan rate of 2.4 μm sec^{-1} and analyzed with Zygo MetroPro software.

The thickness of films cast on silicon coupons from 0.5, 1.0, 1.5, and 2% (w/v) solutions of chitosan is determined (Fig. 3). Chitin film thickness ranges from approximately 3.6 nm for the 0.5% (w/v) chitosan casting solution to 230 nm for the 2% (w/v) solution. Within other constraints it is desirable to maximize film thickness in order to maximize the possible duration of experiments with degradative enzymes. The 2.0% (w/v) solution is difficult to cast consistently because of the high viscosity. Films cast from 1.5% (w/v) solutions are therefore selected for experiments. The average film thickness for chitin thin films cast from 1.5% (w/v) chitosan casting solutions onto the QCM electrodes is 120.0 ± 6.3 nm.

Mass by Quartz Crystal Microbalance

Film mass is measured by QCM.[39] Chitin thin films are prepared on AT-cut quartz crystals with a nominal frequency of 10 MHz (International Crystal Manufacturing, Oklahoma City, OK). The quartz crystals are 20 mm in diameter and 0.167 mm thick, with 100-Å-thick chromium (to enhance gold adhesion), and 1800-Å-thick gold bilayer electrodes. The electrodes on each side of the crystal are of different sizes and are plated prior to purchase. The ground electrode has

[38] F. C. Demarest, *Meas. Sci. Technol.* **9**, 1024 (1998).

[39] K. H. Stellenberger, M. Wolpers, T. Fili, C. Reinartz, T. Paul, and M. Stratmann, *Faraday Discuss.* **107**, 307 (1997).

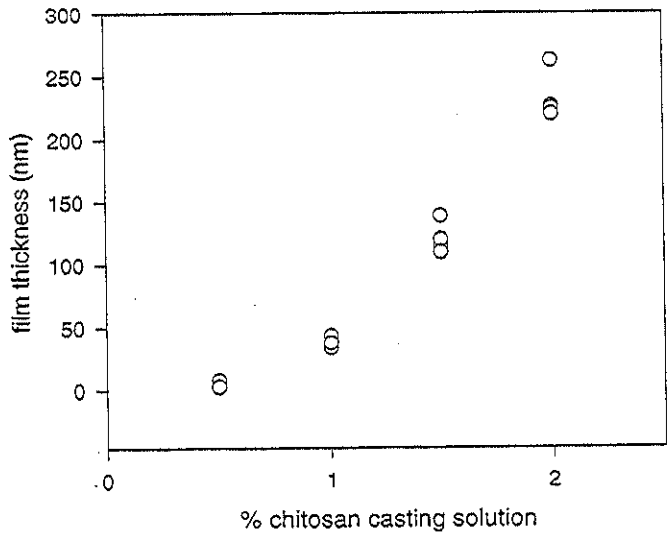


FIG. 3. Thickness of chitin films cast from solutions of various chitosan concentrations.

a diameter of 7 mm; the excited electrode has a diameter of 5 mm. The ground electrode is additionally coated with 1000 Å of silicon dioxide to match the surface chemistry of the solid silica substrata. The crystals are mounted in a spring mount HC-48/u base. A standard laboratory crystal oscillator, model 035360 (International Crystal Manufacturing), is used to excite the quartz crystal. The oscillator is equipped with a BNC output to a frequency counter. A Hewlett-Packard (Palo Alto, CA) 5314A frequency counter is used to measure the resonant frequency changes.

Mass is calculated from the change in frequency of the crystal resonance before and after thin film deposition. Mass measurements are combined with the thickness measurements obtained by profilometry to calculate density of the chitin thin films. The average mass of films is 24.6 ± 0.8 μg cm^{-2}, yielding an average density of 2.05 g cm^{-3}. Preliminary results suggest film thickness may increase as much as 30–40% for every 5° decrease in temperature. This may be caused by an increase in viscosity of the chitosan solutions at lower temperatures.

Intrinsic Background Fluorescence

Microbes attached to opaque materials are typically observed microscopically, using some form of epiillumination. Fluorescence associated with a material can interfere with resolution of micron-sized objects, especially when the underlying

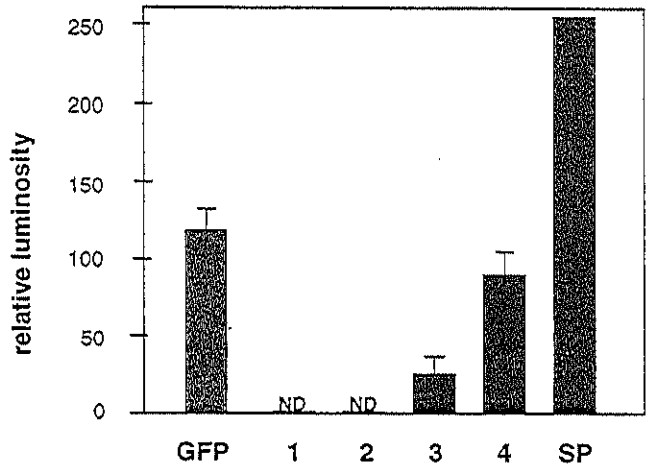


FIG. 4. Intrinsic fluorescence associated with various substrata determined by epiillumination of the sample with excitation at 481 nm and emission at 507 nm. Columns 1–4, chitin films cast from 1, 2, 3, and 4% (w/v) chitosan, respectively. SP, natural squid pen chitin; GFP, representative level of GFP fluorescence from upexpressed S91 cells in a biofilm on a chitin thin film [1.5% (w/v) casting solution] (more detailed information on biofilms is contained in Baty[21] and Baty *et al.*[22,23] ND, Not detected.

substratum exhibits surface features of a similar scale. Figure 4 shows the level of fluorescence emitted from various substrata, using epiillumination (details of microscopy are described below). Relative luminosity is a measure of total pixel brightness normalized to the maximum brightness possible. No detectable fluorescence is observed for the 1 and 2% (w/v) chitosan-cast chitin thin films (exposure of 6 sec and a gain of 4). Films cast from 3 and 4% (w/v) solutions exhibit some fluorescence. The fluorescence of these films is lower than that of natural squid pen chitin. Typical levels of fluorescence emission displayed by the GFP in biofilms of chitinolytic bacteria are shown for comparison. Details are given below.

Crystal Structure

Chitin is found in nature in three crystalline forms depending on whether the polymer chains are arranged in parallel (α-form), antiparallel (β-form), or as a mixture of parallel and antiparallel (γ-form).[40] The α-chitin form is the most abundant, followed by the β-chitin and γ-chitin forms. To determine the crystal structure thin film X-ray diffraction was performed, with inconclusive results. Infrared spectra of the films suggest the β-form (see the next section, on ATR-FTIR).

[40] R. A. A. Muzzarelli, *in* "Chitin" (R. A. A. Muzzarelli, ed.), p. 24. Permagon Press, Oxford, 1977.

Characterization by Attenuated Total Reflection-Fourier Transform Infrared Spectroscopy

The infrared (IR) spectrophotometer is a Nicholet 740. Spectra are collected at 4 cm^{-1} resolution. Interferograms are apodized with a Happ–Genzel function. All spectra are collected in attenuated total reflection (ATR) mode. Briefly, the absorbance of IR within an evanescent field is measured. The field penetrates from the internal reflection element (IRE) into the adjacent medium. The penetration is on the order of 1 μm. IREs are germanium trapezoidal prisms with 45° angles, of dimension 0.2 × 5.0 × 2.0 cm (Harrick Scientific). A horizon cell mirror assembly (Harrick Scientific) is used to guide the IR beam into the prism. Exposure of chitin films to aqueous solutions is performed by inserting the prism into a flow chamber previously described.[20] The flow chamber is specially designed to allow microscopic observation of the surface.

Figure 5 shows an IR spectrum of a chitosan film on the IRE (Fig. 5a) and a spectrum of the corresponding chitin film prepared by acetylation (Fig. 5b). Band assignments are summarized in Table II.[41–46] Spectra are presented in units of wavenumbers (cm^{-1}). The composite band in the region from about 950 to 1200 in the spectra of both the chitin and chitosan films originates from pyranose ring vibrations that are, in general, complex.[41,42] This composite band is similar in structure for both the chitosan and chitin films. Because these vibrational modes involve couplings between many atoms in the pyranose ring, some alteration in band structure is expected on modification of a ring functional group through acetylation.

The most pronounced difference between the chitin and chitosan films is the appearance in the chitin spectrum of a composite band with components at 1660 and 1630 and bands at 1560, 1376, and 1308. These band positions are consistent with spectral changes expected on addition of a methyl group to the primary amine of chitosan via a secondary amide linkage (acetylation). The split of the amide I band into composite bands at 1630 and 1660 may be the result of hydrogen bonding of a proportion of the amide linkages, as is described frequently for proteins, with the band at 1630 resulting from a downshift in frequency due to hydrogen bonding of the carbonyl group.[45] With this assumption, using band areas of the component bands, the proportion of amide linkages involved in hydrogen bonding is 60%. The spectrum of cast films resembles β-chitin from *Oligobrachia ivanovi* tube

[41] J. J. Cael, K. H. Gradner, J. L. Koenig, and J. Blackwell, *J. Chem. Phys.* **62**, 1145 (1975).
[42] J. J. Cael, K. H. Gradner, J. L. Koenig, and J. Blackwell, *Biopolymers* **14**, 1885 (1975).
[43] C. J. Pouchert, "The Aldrich Library of Infrared Spectra," 2nd Ed., p. 1576. Aldrich Chemical Company, Milwaukee, Wisconsin, 1978.
[44] J. Blackwell, K. D. Parker, and K. M. Rudall, *J. Mol. Biol.* **28**, 383 (1967).
[45] M. Jackson and H. H. Mantsch, *Crit. Rev. Biochem. Mol. Biol.* **30**, 95 (1995).
[46] T. Miyazawa, T. Shimanouchi, and S.-I. Mizushima, *J. Chem. Phys.* **29**, 611 (1958).

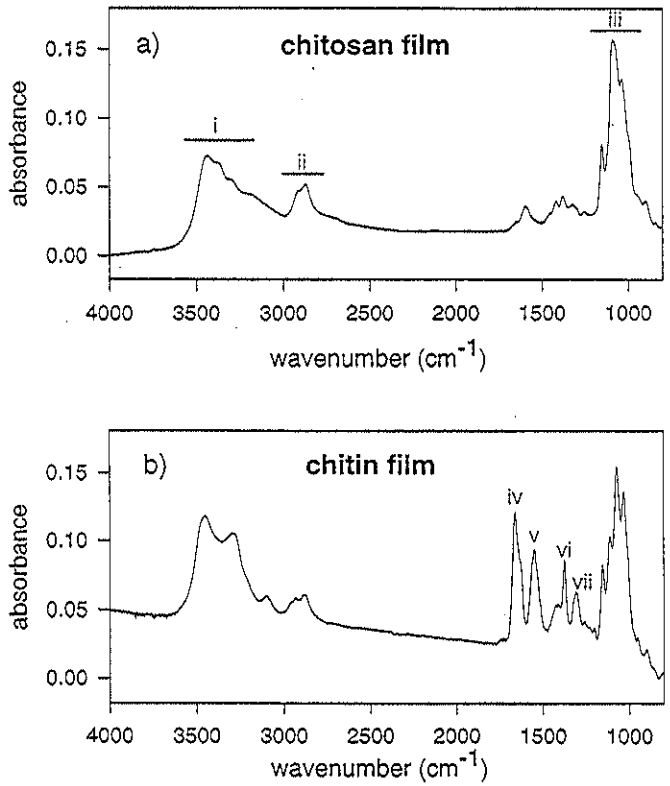


FIG. 5. Spectra of a thin film of chitosan (a) and chitin (b) acquired by ATR-FTIR. Spectral features labeled with roman numerals are referred to in Table II and in text. For structures see Fig. 1.

in some respects.[44] Bands having corresponding positions are evident at 3453, 3291, 1659, approximately 1635 (shoulder), 1550, 1376, 1202, 1154, 1071, 1030, and 953. The relative amplitudes of the main band and shoulder at, respectively, 1659 and 1635 are reversed. The position of the hydrogen-bonded amide I band at 1630 suggests that the pattern of hydrogen bonding resembles β-chitin more closely than α-chitin.[44] The protocol used to deacetylate the chitosan completely removes all acetyl groups according to the FTIR spectra, because there is no indication of amide I and II bands in the chitosan films. The band at 1600 in the chitosan spectrum may originate from NH_2 deformations of the primary amine group.[43]

There are some differences in the chitosan and chitin spectra in the region between 3000 and 3500. This region contains vibrational modes associated with N–H stretches of both primary amines and amides and also O–H stretches. Therefore, acetylation is expected to cause changes in band structure, and both chitosan and

TABLE II
BAND ASSIGNMENTS FOR SPECTRA PRESENTED IN FIG. 5

Figure label	Assignment	Ref.
i	NH stretch of amines and amides, OH stretch	41–43
ii	CH stretch	44
iii	Pyranose ring vibrations	41,42
iv	Amide I	45,46
v	Amide II	45,46
vi	CH bending mode of CH_3	46
vii	Amide III	46

chitin are expected to have overlapping bands in this region. It was not possible to make precise assignments for components of these composite bands.

ATR-FTIR enables direct detection of the acetylation process of chitosan films. Acetylation changes the band structure of the pyranose ring vibrations and the CH stretch region between 2800 and 3000 only slightly, whereas the amide I and II peaks are present only in the chitin films. Therefore, the ratio of the amide I or II bands to either the composite band associated with the pyranose ring, or that associated with the CH stretches, can be used to determine the extent of relative acetylation. This is shown in Fig. 6, where the region of pyranose ring vibrations was used for the normalization. Acetylation of the film is completed within about 24 hr of exposure to acetic anhydride.

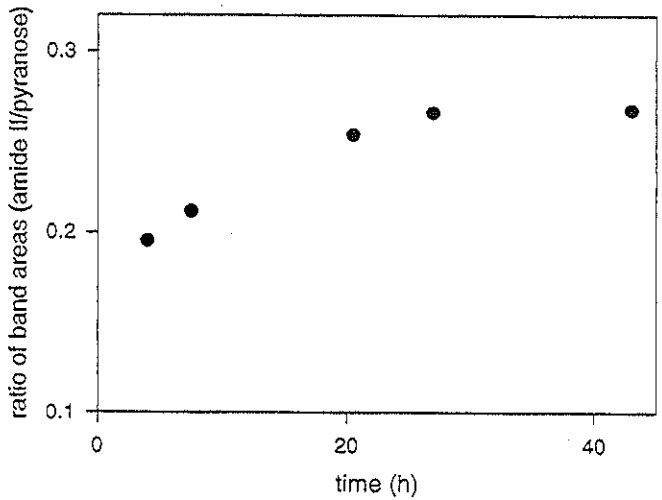


FIG. 6. Changes in the ratio of the amide II band (1504–1601) to the composite band originating from pyranose ring vibrations (981–1183) for times of acetylation in acetic anhydride.

Characterization of Chitinolytic Activity in Biofilms

The characterization of biofilms is described in three publications.[21-23]

Flow Cell

Biofilms are cultured on coupons placed in laminar flow cells (LFCs), based on a previous design.[47] LFCs are constructed of Teflon (McMaster Carr, Los Angeles, CA). The flow channel is 0.8 mm deep, 12 mm wide, and 48 mm in length. Two 1 × 1 cm squares are recessed, in series, into the floor of each LFC to accommodate silicon, chitin, or squid pen chitin coupons. A no. 2 coverslip (24 × 60 mm) is used as the viewing window and is sealed against the Teflon, using an oversized Viton gasket and an aluminum coverplate. Teflon influent and effluent lines are connected with Chemfluor PTFE gas fittings (Cole Parmer, Vernon Hills, IL). The LFCs are connected with silicon tubing (Cole Parmer) to both an air-sparged, continuously stirred tank reactor and a 20-liter carboy of artificial seawater. Influent lines are fed through a Buchler 12 roller Multistatic pump (Cole Parmer). The flow dynamics in the LFCs are characterized by injecting a slug dose of crystal violet dye. The flow of the crystal violet moved in a plug flow fashion, suggesting laminar flow of the aqueous phase across the coupons. The flow rate of artificial seawater through each LFC is 0.5 cm^3 min^{-1}, corresponding to a fluid flow velocity of 75 m day^{-1}. The shear stress at the surface under these conditions is equivalent to 0.004 pN μm^{-2} of force. The residence time of the bulk aqueous phase flowing through the LFCs is 55.3 sec.

Transcriptional Activity

GFP fluorescence is used to monitor the promoter activity of *chiA*. *Pseudoalteromonas* sp. strain S91 is derived from the wild-type strain S9, a chitinolytic marine bacterium isolated from the surface waters of Botany Bay, New South Wales, Australia in 1981.[48] Strain S91 contains plasmid pDSK519 with a complete chitinase gene (*chiA*) and a truncated chitin-binding gene (*chiB*).[49] Strain S91 is streptomycin resistant and the plasmid confers kanamycin resistance. The *gfp* gene is under the control of both the *chiA* and *chiB* promoters.[50,51] This *gfp* gene encodes the GFPmut2 variant.[52] GFPmut2 excites optimally at 481 nm with an emission maximum at 507 nm.

[47] D. G. Davies and G. G. Geesey, *Appl. Environ. Microbiol.* **61**, 860 (1995).
[48] B. Humphrey, S. Kjelleberg, and K. C. Marshall, *Appl. Environ. Microbiol.* **45**, 43 (1983).
[49] N. T. Keen, S. Tamaki, D. Kobayashi, and D. Trollinger, *Gene* **70**, 191 (1988).
[50] S. Stretton, S. Techkarnjanaruk, A. M. McLennan, and A. E. Goodman, *Appl. Environ. Microbiol.* **64**, 2554 (1998).
[51] S. Techkarnjanaruk and A. E. Goodman, *Microbiology* **145**, 925 (1999).
[52] B. P. Cormack, R. H. Valdivia, and S. Falkow, *Gene* **173**, 33 (1996).

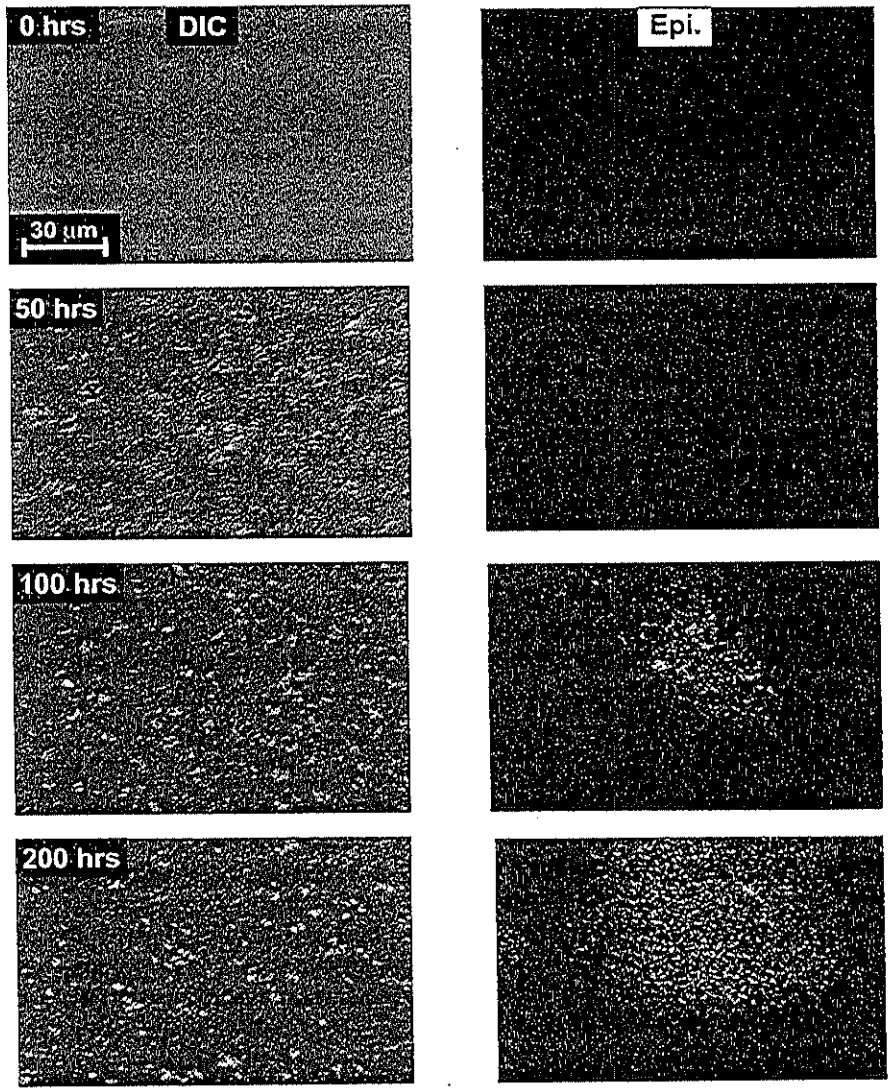


FIG. 7. DIC and epifluorescence (Epi.) micrographs of S91 biofilms on chitin films at various times after flow cell inoculation.

Micrographs of biofilms of S91 cultured on chitin thin films are shown in Fig. 7. DIC is used to visualize total cells, whereas epifluorescence is used to visualize the subset of the population expressing chitinolytic genes.

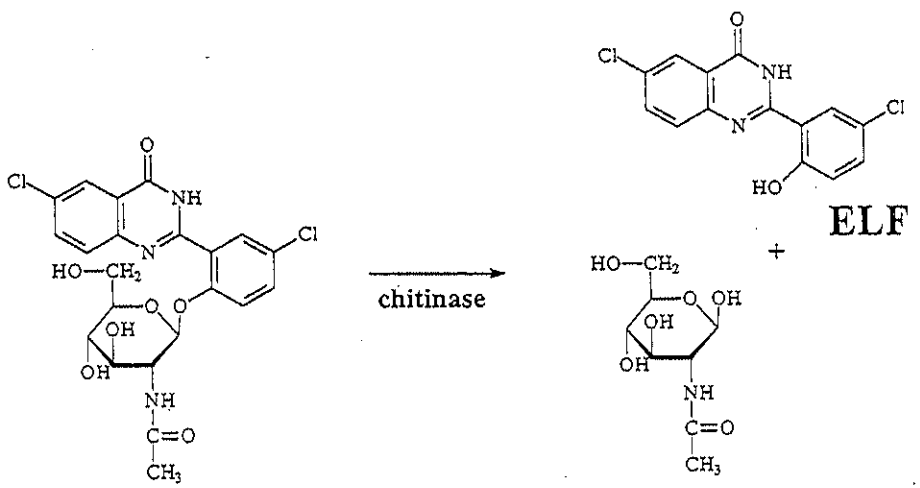


FIG. 8. Enzymatic hydrolysis of ELF-NAG that produces the fluorescent precipitating compound (ELF).

Catalytic Activity

The ELF-NAG fluorogenic probe is used to visualize regions of the coupons exhibiting chitinolytic activity. Enzymatic hydrolysis with pure *Streptomyces griseus* chitinase yields a bright yellow–green precipitate with the excitation (360 nm) and emission (540 nm) wavelengths of the fluorophore, 2-(2′-hydroxy-5′-chloro phenyl)-6-chloro-4(3*H*)-quinazolinone (ELF). The reaction is shown in Fig. 8.

ELF-NAG is dissolved in dimethyl sulfoxide at a concentration of 10 m*M*. A 50 μ*M* solution of ELF-NAG is prepared by adding a 10-μl volume of the 10 m*M* stock solution to 2.0 ml of artificial seawater. The mixture is filtered through a 0.2-μm PTFE Millipore membrane to remove any residual crystals, injected into the LFC, incubated in the dark at 20° for 1 hr, and rinsed from the LCF. Areas where the probe has precipitated onto the surface are visualized by epifluorescence microscopy.

ELF-NAG and GFP excite in different ranges. This enables their discrimination in the same field of view. Figure 9 (see color insert) shows image overlays of three types of images. DIC images allow visualization of total cells; epifluorescent images acquired at different excitation wavelengths allow visualization of the level of promoter activity associated with individual cells, and the location of extracellular enzymatic activity, indicated by precipitation of the ELF fluorogenic

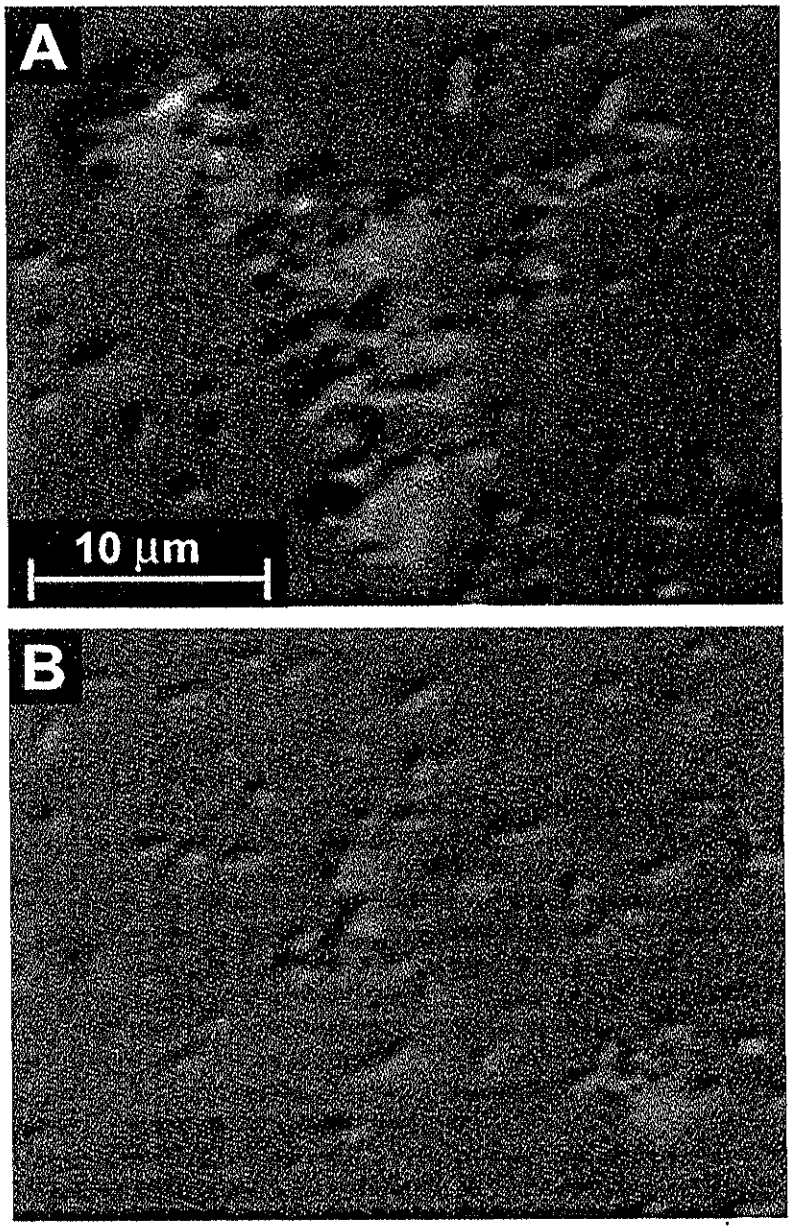


FIG. 9. Color-enhanced, DIC epifluorescence image overlays showing *chiA* upexpression (green pseudocolor) and ELF fluorescence (red pseudocolor) indicating chitinase activity. (A) Chitin film; (B) silicon substratum.

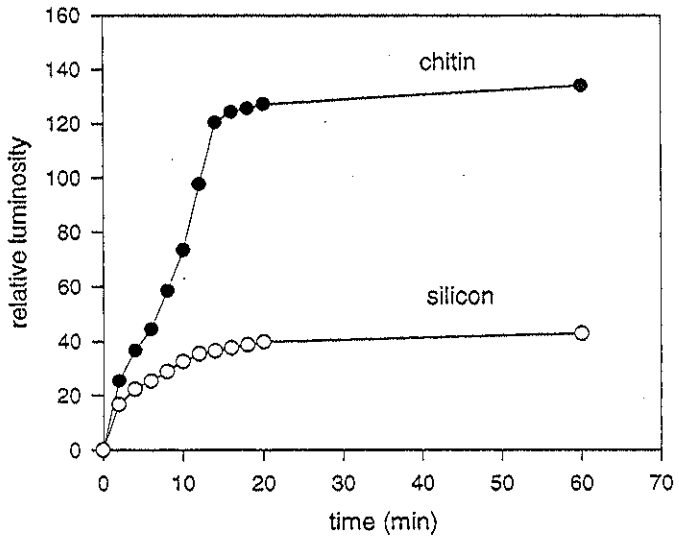


FIG. 10. Kinetics of appearance of fluorescence after exposure of S91 biofilms on chitin films (filled circles) and silicon coupons (empty circles) to the ELF fluorogenic probe. No fluorescence was detected from the abiotic control (data not shown). Fluorescence was detected by epifluorescence microscopy of biofilms cultured for 100 hr.[21–23]

probe onto the substratum. The images reveal that chitinase activity is closely linked to *chiA* upexpressed cells. However, not all cells that were *chiA* upexpressed produced active chitinase.

Epifluorescence microscopy and image analysis are used to monitor the relative rate of conversion of ELF-NAG to the ELF by measuring the relative luminosity of the enzyme active sites on chitin, silicon, and the abiotic silicon control (Fig. 10). The fluorescent product can be detected in as little as 2 min within a surface-associated population of S91 actively involved in chitin degradation. Even on a chitin-free silicon surface S91 exhibits some chitinase activity. The reactivity of ELF-NAG slows considerably by 20 min after inoculation of the enzyme substrate. It is possible that ELF is forming a physical barrier around the active site of the chitinase as it precipitates, thus limiting the mass transport of ELF-NAG to the enzyme.

Substrate Degradation Using Attenuated Total Reflection-Fourier Transform Infrared Spectroscopy

ATR-FTIR can be used to monitor the kinetics of degradation of a chitin film exposed to a solution of chitinase in a flow chamber. Difference spectra are computed as the ratio of all spectra acquired during the time course, to a

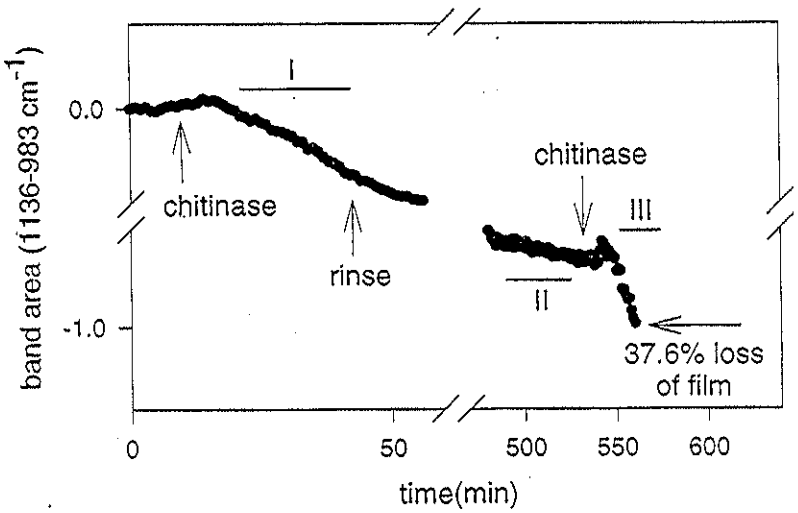


FIG. 11. Changes in negative area of the down-going band associated with the pyranose ring computed from ATR-FTIR difference spectra. Times of introduction of chitinase solution and rinse with PB are indicated. Roman numerals indicate intervals of computation of rates of degradation presented in Table III. Note that the time scale is condensed after the break. Loss of the film was computed on the basis of measurement of dried films as described.

spectrum taken immediately after the flow chamber is filled with buffer. As the film degrades, down-going bands appear in difference spectra as chitin is washed from the interface. The most prominent down-going bands are in the region of the pyranose ring vibrations.

For ATR-FTIR experiments a specially designed flow cell described previously is used.[20] The flow cell allows both ATR-FTIR measurements and microscopic observation of the substratum. The flow rate is 0.5 ml/min. Chitinase is from *S. griseus* (Fluka, Milwaukee, WI). The enzyme activity reported by the distributor is 1 μmol of *N*-acetylglucosamine per minute released per unit (U) at pH 4.4 at 37° with colloidal chitin as substrate (70 U/g). Chitinase solutions are made up in phosphate buffer (PB) consisting of sodium phosphate (pH 4.4) at 1 g/liter). All experiments are conducted at room temperature (approximately 20°).

Figure 11 shows the increase in negative area of down-going bands in the region from 983 to 1136 (cm^{-1}) as a chitin film is rinsed with PB and then exposed to chitinase (0.01 mg/ml). There is a significant delay between the time the enzyme is introduced into the flow chamber and the first indication that chitin is being lost from the substratum. The enzyme must diffuse to the substratum and bind to the chitin substrate before chitin degradation can begin. There may also be a significant delay between initiation of enzyme activity and significant chitin removal from the

TABLE III
RATES OF DEGRADATION OF CHITIN FILM BY CHITINASE

Time period (min)[a]	Rate of loss (μg/min)
15–40 (I)[a]	0.280
490–530 (II)	0.0230
548–560 (III)	0.3025

[a] See Fig. 11.

region of penetration of the evanescent field. The slight increase in the band area during this time period may result from a change in structure of the chitin film as the chitinase adsorbs and begins hydrolyzing the glycosidic linkages. The chitin film continues to degrade after the chitinase is rinsed from the flow chamber, with the rate of loss of the film only decreasing gradually. This may be due in part to chitin degradation associated with adsorbed chitinase that is only rinsed from the surface slowly as the film continues to decompose. The film is rinsed for approximately 8 hr (break in Fig. 11 ordinate and abscissa) and then exposed once again to a PB solution of chitinase (0.01 mg/ml). The film is then allowed to dry and a spectrum is acquired in air (without the flow chamber). According to the decrease in area of the composite band of the pyranose ring vibrations 37.6% of the chitin film is removed during the entire period of the experiment. Rates of degradation of the film during three time intervals were computed (indicated in Fig. 11). The slope of the linear regression for each time interval yields a rate in terms of change in area of the down-going band per minute. Area of the down-going band is converted to mass of the film by using the nominal density and thickness of the films prepared from a 1.5% (w/v) solution of chitin. This yields a rate of degradation in terms of mass of chitin lost from the film per minute. These data are presented in Table III for the three time intervals.

The first interval in Table III corresponds to the first exposure of the film to chitinase. The second interval is the rate of degradation after an 8 hr rinse period. This rate is an order of magnitude less than the rate of degradation during the first exposure to chitinase at 0.01 mg/ml. When the film is exposed a second time to chitinase at 0.01 mg/ml, the rate is increased to a level slightly higher than that of the first interval. The residual rate of degradation of the chitin film, measured for the rinse period between the first and second exposure to chitinase, makes up the balance of the difference between the rates for the first and second time intervals. This implies that there are two processes of degradation occurring during the second exposure to chitinase. Exposure to chitinase presumably disrupts the film by breaking glycosidic linkages and releasing monomeric *N*-acetylglucosamine. It may be that the film is destabilized by the first exposure to chitinase, and that loss of the film proceeds gradually even in the absence of the enzyme. For example,

the packing of the chains may be disrupted by chitinase, allowing portions of the film to detach during exposure to flowing buffer even though the chitinase activity has become negligible.

The rates of degradation of the chitin film are comparable to the rate expected for degradation of colloidal chitin by chitinase from *S. griseus*. Assuming that activity is proportional to units of enzyme, the estimated activity of a 0.01-mg/ml solution of chitinase is 7×10^{-10} mol of *N*-acetylglucosamine per minute or 0.15 μg/min. The rates would not be expected to be exactly the same because experimental conditions differ. Most pronounced differences are the temperature (20 vs 37°), and the fact that enzyme is continually replenished in the present experiments by flowing the solution over the surface.

Synthesis of ELF-97-*N*-acetyl-β-D-glucosaminide Fluorogenic Probe

At the time the methodologies described here were being developed ELF-NAG was not available commercially. Therefore, a synthesis was designed and executed.[21] ELF-NAG is currently available (Molecular Probes, product E-22011). The major steps for probe synthesis are outlined in Fig. 12.

All organic chemicals are purchased from Aldrich (Milwaukee, WI), except for 5-chloro-2-aminobenzoic acid, which is purchased from Arcos Organics (Pittsburgh, PA). Nuclear magnetic resonance (NMR) spectra are obtained on a Bruker YLIV370.040.

Compound **I** (Fig. 12) (2-acetamido-2-deoxy-β-D-glucopyranose-1,3,4,6-tetraacetate) is prepared as follows. The O-acetylation and halogenation of *N*-acetyl-β-D-glucosamine are performed by a modification of published methods.[53] *N*-Acetyl-β-D-glucosamine (20 g) is dried and triturated and slowly dissolved in a mixture of acetic anhydride (100 ml) and concentrated sulfuric acid (13.0 ml) on ice. The mixture is held for 24 hr at room temperature and then poured into a cold solution of anhydrous sodium acetate (82 g) in water (520 ml) while stirring. The solution is then extracted with chloroform (3 × 100 ml). The chloroform extracts are combined and washed successively in ice-cold water (2 × 200 ml), ice-cold saturated sodium bicarbonate (3 × 200 ml), and ice-cold water (2 × 200 ml). The chloroform is removed with a rotary evaporator and dried over anhydrous sodium sulfate. The product is then further dried under reduced pressure over phosphorous pentoxide. The final product, 2-acetamido-2-deoxy-β-D-glucopyranose-1,3,4,6-tetraacetate (Fig. 12, compound **I**), is then dissolved and recrystallized from ethyl acetate.

The compound 2-acetamido-2-deoxy-β-D-glucopyranose-1,3,4,6-tetraacetate (10.0 g) is dissolved in a solution of acetic acid (120 ml) and acetic anhydride

[53] T. Inabe, T. Ohgushi, Y. Iga, and E. Hasegawa, *Chem. Pharm. Bull.* **32**, 1597 (1984).

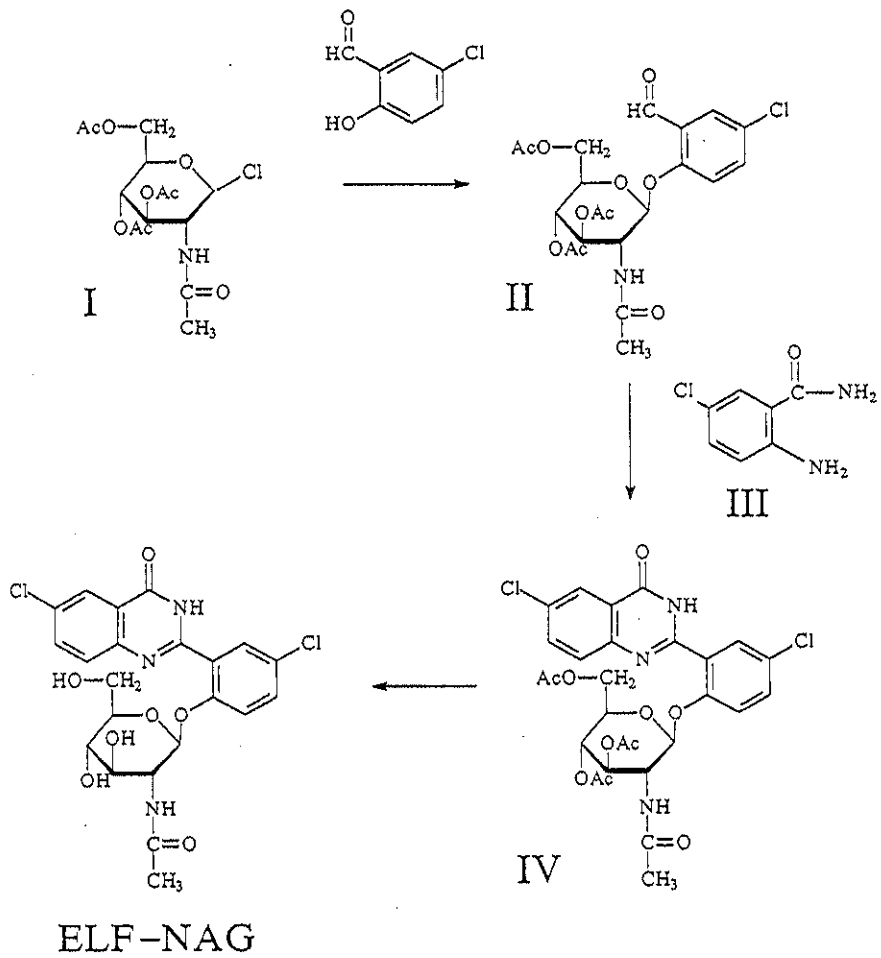


FIG. 12. Major steps in probe synthesis. Roman numerals refer to compounds mentioned in text. For simplicity hydrogen atoms are not shown. Ac, Acetyl group.

(1.0 ml) and cooled to 4°. The mixture is then saturated with dry hydrochloride gas, using a fine glass air stone while stirring on ice. The reaction mixture is then tightly sealed and held at room temperature for 48 hr while stirring. The reaction mixture is poured into chloroform (400 ml) and washed successively in ice-cold water (2 × 200 ml), ice-cold saturated sodium bicarbonate (3 × 200 ml), and ice-cold water (2 × 200 ml). The chloroform is removed with a rotary evaporator to a volume of 10–12 ml. The remaining solvent is removed under a gentle stream of dry nitrogen. The product is dried over anhydrous sodium sulfate and

then further dried under reduced pressure over phosphorous pentoxide. The final product, 1-chloro-2-acetamido-2-deoxy-*b*-D-glucopyranose-3,4,6-tetraacetate, is redissolved and recrystallized from chloroform–diethyl ether.

Compound **II** (Fig. 12) [4-chloro-2-formylphenyl-(2-acetamido-2-deoxy-β-D-glucopyranose-3,4, 6-tetraacetate)] is prepared as follows. Compound **I** (3.7 g) and 4-chlorosalicylaldehyde (2.5 g) are dissolved in anhydrous dichloromethane (50 ml). To the solution is added at once Ag_2CO_3 (4.4 g) and 3-Å molecular sieves (5 g). 2,4,6-Collidine (2.1 ml) is added, dropwise, with stirring. The resulting mixture is stirred in the dark, at room temperature for 4 days under dry argon protection, and then diluted with chloroform (150 ml). The mixture is filtered through a pad of Celite diatomaceous earth and the residue is washed with chloroform (3 × 50 ml). The combined filtrates are washed successively with 1 *M* HCl solution (2 × 250 ml), water (1 × 250 ml), 0.1 *M* $Na_2S_2O_3$ solution (2 × 250 ml), saturated $NaHCO_3$ solution (2 × 250 ml), and water (2 × 250 ml). The organic layer is dried over anhydrous $MgSO_4$, and evaporated *in vacuo* to give an off-white solid. The crude material is purified on a silica gel column, using a gradient elution of chloroform and acetonitrile, to yield the final product, 4-chloro-2-formylphenyl-(2-acetamido-2-deoxy-β-D-glucopyranose-3,4,6-tetraacetate) (Fig. 12, compound **III**), a colorless solid (3.7 g; yield, 84%).

Compound **III** (Fig. 12) (4-chloroanthranilamide) is prepared by methods described previously.[54] 5-Chloro-2-aminobenzoic acid (anthranilic acid) (5.0 g) is dissolved in tetrahydrofuran (100 ml). The mixture is cooled to 0° and saturated with dry ammonia gas for 2 hr while stirring. The reaction mixture is then allowed to warm to room temperature and is stirred overnight. The tetrahydrofuran is removed by rotary evaporation. The product, 4-chloroanthranilamide, is recrystallized from toluene.

Compound **IV** (Fig. 12) (4-chloro-2-[2′-(6″-chloro-4(3*H*)-quinazolinonyl)]-phenyl-2-acetamido-2-deoxy-β-D-glucopyranose-3,4,6-tetraacetate) is prepared as follows. Compound **II** (741 mg), compound **III** (297 mg), and *p*-toluenesulfonic acid (20 mg) are dissolved in anhydrous methanol (30 ml) and stirred at room temperature for 2 hr. The reaction mixture is then refluxed for another 1 hr. The resulting solution is cooled to 0° and 2,3-dichloro-4,5-dicyano-1,4-benzoquinone (386 mg) is added in three portions over the course of 30 min. The mixture is stirred at 0° for 2 hr, and evaporated *in vacuo* to give a brown solid. The solid is washed with benzene (5 × 50 ml) to remove the hydroquinone formed during the reaction. The resulting residue is dissolved in methanol and precipitated by ether. The crude material is purified on silica gel, using a gradient elution of chloroform and methanol to yield the final product, 4-chloro-2-[2′-(6″-chloro-4(3*H*)-quinazolinonyl)]-phenyl-2-acetamido-2-deoxy-β-D-glucopyranose-3,4,6-tetraacetate, a colorless solid, (874 mg; yield, 76%).

[54] Z. Diwu, Y. Lu, R. H. Upson, M. Zhou, D. H. Klaubert, and R. P. Haugland, *Tetrahedron* **53**, 7159 (1997).

Compound **IV** is deprotected to yield the enzyme substrate ELF-97-*N*-acetyl-β-D-glucosaminide. Compound **IV** (800 mg) is dissolved in anhydrous methanol (10 ml) and cooled to 0°. Freshly prepared 0.1 *M* sodium methoxide in anhydrous methanol (3 × 0.1 ml) is slowly added to the solution in three portions over 2 hr under dry argon protection. The solution is stirred at 0° for 2 hr, warmed to room temperature, and stirred for 4 hr. The reaction mixture is then diluted with methanol (50 ml), and acidified (pH 6.0) with Amberlite IRC-50 ion-exchange resin (H^+ form). The mixture is filtered, and the resin is washed with methanol (2 × 25 ml). The combined filtrate is evaporated *in vacuo* to give an off-white solid. The crude material is dissolved in methanol, and precipitated by ether to afford the final product, ELF-97-*N*-acetyl-β-D-glucosaminide, an off-white solid (1.4 g; yield, 94%); ^{1}H-NMR (DMSO-d_6): 12.20 (1H, s); 8.1 (1H, s); 7.85, 7.28 (2H, dd); 7.70, 7.47 (2H, dd); 7.60 (1H, s); 5.10 (1H, m); 5.00 (1H, m); 4.92 (1H, m); 4.60 (1H, m); 4.30 (1H, m); and 3.10–3.90 ppm (9H, m).

Summary

Extracellular enzymes produced by bacterial biofilms tend to become an integral, permanent part of the biofilm/substratum system. Thus, characterizing extracellular enzyme activity is an essential component of understanding biofilm ecology. Methods have been presented for characterizing three aspects of extracellular enzyme activity in biofilms: promoter activity of the structural gene, local catalytic activity, and kinetics of collective substrate degradation. The abundance of intracellular transcript derived from a structural gene is only indirectly related to the magnitude of catalytic activity of the corresponding enzyme. This relationship may be particularly tenuous in the case of extracellular enzymes, which must be transported out of the cell in order to become active. Fluorogenic substrates that allow direct detection of an increasingly greater variety of enzyme activities are becoming available. There are technical problems, originating from surface roughness and intrinsic fluorescence, associated with microscopic examination of biofilms on natural materials. Thin films provide one option for acquiring data about biofilms colonizing relevant materials.

Acknowledgments

This work was sponsored by the National Science Foundation (OCE 9720151, Geesey and EEC 8907039, cooperative agreement), Office of Naval Research grant N00014-97-1-1062, and National Institute of Dental and Craniofacial Research grant N01-DE-62611. A portion of this work was performed in the Environmental Molecular Sciences Laboratory, a national scientific user facility sponsored by the Department of Energy's Office of Biological and Environmental Research located at Pacific Northwest National Laboratory.